Journal of Magnetism and Magnetic Materials 321 (2009) 3758–3763

Contents lists available at ScienceDirect

Journal of Magnetism and Magnetic Materials

journal homepage: www.elsevier.com/locate/jmmm

Magnetostatic interactions and forces between cylindrical permanent magnets

David Vokoun [a,*], Marco Beleggia [b,1], Luděk Heller [a], Petr Šittner [a]

[a] Institute of Physics ASCR, v.v.i., Prague, Czech Republic
[b] Institute for Materials Research, University of Leeds, Leeds LS2 9JT, United Kingdom

ARTICLE INFO

Article history:
Received 19 February 2009
Received in revised form
24 June 2009
Available online 17 July 2009

Keywords:
Cylinder
Force measurement
Magnetostatic
Permanent magnet

ABSTRACT

Permanent magnets of various shapes are often utilized in magnetic actuators, sensors or releasable magnetic fasteners. Knowledge of the magnetic force is required to control devices reliably. Here, we introduce an analytical expression for calculating the attraction force between two cylindrical permanent magnets on the assumption of uniform magnetization. Although the assumption is not fulfilled exactly in cylindrical magnets, we obtain a very good agreement between the calculated and measured forces between two identical cylindrical magnets and within an array of NdFeB cylindrical magnets.

1. Introduction

Attraction forces between permanent magnets are established by magnetostatic interactions. When modeling magnetostatic interactions in an array of magnetic elements, it is common practice to initiate the energy computation by considering interactions among elementary magnetic dipoles. This approximation is acceptable when elements are distributed at large enough distances from one another. However, when dealing with permanent magnets utilized as, e.g., magnetic fasteners, modeling near-contact attractive magnetostatic forces requires a more advanced treatment that takes into account shape effects. Magnetostatic interactions among elements of various regular shapes are examined in analytical fashion in [1–4].

In a previous study [5], we introduced a semi-analytical formula for the magnetostatic interaction between two uniformly magnetized cylindrical elements of equal radius. In the present study, we first review briefly our subsequent achievement [6] of recasting the same formula in fully analytical form by means of elliptic integrals. Then, keeping the assumptions of uniform magnetization and equal cylinder radius, we calculate the attraction force between two groups of cylindrical permanent magnets where we assume that all the magnets are axially magnetized (the direction of the vector of magnetization is parallel with the axis of symmetry in each cylinder) and all the cylinder axes are parallel. Working with 1–4 permanent cylindrical magnets in each group we then compare our formula to experimental data obtained by pulling apart two permanent magnet sets while measuring continuously both the distance between the sets and force. A force approximation for two distant permanent cylindrical magnets is also derived. The comparison between the force approximation and the force calculated on the basis of the cylinder parameters is shown for various magnet distances.

Another formula for the determination of the attraction force between two cylindrical magnets is introduced by Agashe and Arnold [7]. Their formula is similarly based on the assumption of uniform magnetization in the axial direction while using a magnetic field approximation for a cylindrical magnet [8]. We show that for the contact force of two identical cylindrical magnets, the formula from Ref. [7] and our expression give similar force values in the range of aspect ratios spanned by the experiments.

2. Expressions for magnetostatic interaction energy and attraction forces

The attraction force between sets of magnets can be derived from the total magnetostatic interaction energy of the system E according to

$$\vec{F} = -grad(E). \quad (1)$$

We assume that all cylindrical magnets are made of the same material characterized by saturation magnetization M. As for the geometry, the cylindrical magnets are of equal radius R and are

* Corresponding author.
E-mail address: vokoun@fzu.cz (D. Vokoun).
[1] Now at: Center for Electron Nanoscopy, Technical University of Denmark, DK-2800 Kgs. Lyngby, Denmark.

0304-8853/$ - see front matter © 2009 Elsevier B.V. All rights reserved.
doi:10.1016/j.jmmm.2009.07.030

magnetized uniformly along the cylinder axis of symmetry. In our derivations, we do not allow any magnetization vector rotation during the interaction, which may be thought as the effect of a strong intrinsic axial anisotropy induced by the manufacturer, nor do we consider sets of magnets with rotated axes of symmetry.

2.1. Two cylindrical permanent magnets with a common axis

In this case, either set consists of just one cylindrical magnet. The interacting cylinders are sketched in Fig. 1a. If we choose the coordinate system with the z-axis along the cylinders axis, then the attraction force acts only along z and can be expressed according to (1) as follows:

$$F_z = -\frac{\partial E}{\partial Z} = 2\pi\mu_0 M^2 R^3 \frac{\partial J_d}{\partial Z}, \tag{2}$$

where μ_0 is the permeability of vacuum and J_d the dipolar coupling integral defined in [5]. Following the computational method described in [1] the dipolar coupling integral J_d can be expressed as

$$J_d(\tau_1,\tau_2,\varsigma) = 2\int_0^{+\infty} \frac{J_1^2(q)}{q^2}\sinh(q\tau_1)\sinh(q\tau_2)e^{-q\varsigma}\,dq, \tag{3}$$

where $\tau_i = t_i/(2R)$, $i = 1, 2$, are the aspect ratios of the two cylinders, $\zeta = Z/R$ is the reduced distance between the centers of the two cylinders (see Fig. 1a) and $J_1(q)$ is a modified Bessel function of the first kind. On the assumption that the integral in (3) converges uniformly, we may exchange the order of integration and derivation arriving at

$$F_z = -8\pi K_d R^2 \int_0^{+\infty} \frac{J_1^2(q)}{q}\sinh(q\tau_1)\sinh(q\tau_2)e^{-q\varsigma}\,dq, \tag{4}$$

where we have introduced the magnetostatic energy constant $K_d = \mu_0 M^2/2$ for convenience of notation. Eq. (4) is the attraction force acting in the axial direction, while no attraction forces exist in x and y. As for numerical evaluation of the integral in (4) it is convenient to convert the integral to a more manageable form. The integral is of Lipschitz–Hankel type [9] and may be expressed analytically in terms of a combination of elliptic integrals. Following the notation in [10] we denote the integral as

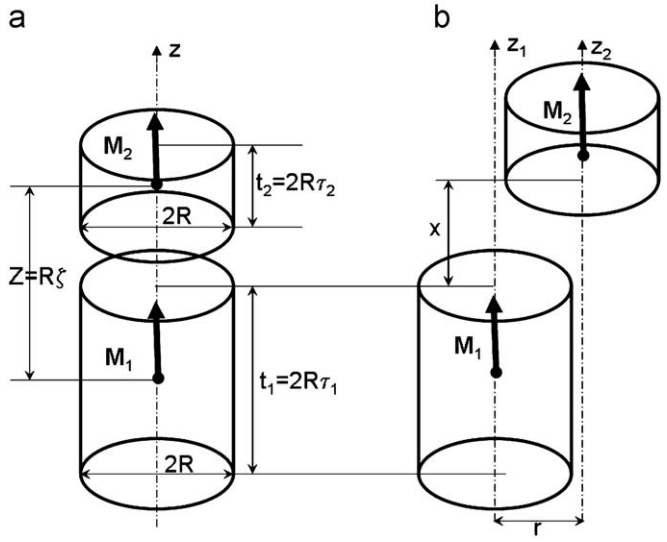

Fig. 1. A scheme of the two interacting cylindrical permanent magnets: (a) with a common axis and (b) with parallel but displaced axes. R is the magnets radius, τ_i their aspect ratios, Z the distance between their centers, M_i their magnetizations, r their lateral displacement, and x the gap between the poles.

$$A^{\alpha}_{\mu\nu}(a,b,c) = \int_0^{\infty} x^{\alpha-1}e^{-ax}J_{\mu}(bx)J_{\nu}(cx)\,dx. \tag{5}$$

After rewriting the hyperbolic function in terms of exponentials, the integral in (4) can be expressed as a combination of terms of type $A^0_{11}(\omega,1,1)$ as follows:

$$F_z = -2\pi K_d R^2 \sum_{i,j=-1}^{1} i\cdot j\cdot A^0_{11}(\varsigma + i\tau_1 + j\tau_2, 1, 1). \tag{6}$$

According to [9]

$$A^0_{11}(\omega,1,1) = \frac{\omega}{\pi k_1}E(k_1^2) - \frac{(2+0.5\omega^2)k_1\omega}{2\pi}K(k_1^2) + \frac{1}{2}, \tag{7}$$

where $k_1^2 = 4/(4+\omega^2)$, and K and E are complete elliptic integrals of the first and the second kind, respectively. It is worth noting that the integral in (3) can be also expressed as combination of complete elliptic integrals using the following relations:

$$J_d = 2\sum_{i,j=-1}^{1} i\cdot j\cdot A^{-1}_{11}(\varsigma + i\tau_1 + j\tau_2, 1, 1), \tag{8}$$

$$A^{-1}_{11}(2\omega,1,1) = \frac{4\sqrt{1+\omega^2}}{3\pi}[(1-\omega^2)E(k_2) + \omega^2 K(k_2)] - \omega, \tag{9}$$

where $k_2^2 = 1/(1+\omega^2)$.

Using (6) and (7) we may calculate the contact force of two identical cylindrical magnets. The contact force (F_0) between two magnets is defined as the attraction force with zero axial and lateral gaps between the magnets. From Fig. 1, we can see that zero gap corresponds to $\zeta = 2\tau$ and $\tau = \tau_1 = \tau_2$. Substituting $\zeta = 2\tau$ in (6) and using (7) and the fact that $A^0_{11}(0,1,1) = 0.5$ we arrive at

$$F_0 = -8K_d R^2 \tau\left\{\frac{1}{l_1}[E(l_1^2) - K(l_1^2)] - \frac{1}{l_2}[E(l_2^2) - K(l_2^2)]\right\}, \tag{10}$$

where $l_1 = 1/\sqrt{1+4\tau^2}$ and $l_2 = 1/\sqrt{1+\tau^2}$. Eq. (10) can be also transformed into a series in powers of l_1 and l_2

$$F_0 = -4\pi K_d R^2 \tau \sum_{n=1}^{\infty} \frac{2n}{2n-1}\left[\frac{(2n-1)!!}{(2n)!!}\right]^2 (l_2^{2n-1} - l_1^{2n-1}). \tag{11}$$

The sum in (11) converges quickly for large aspect ratios τ, giving fast and reasonably accurate estimates of contact forces between two long cylinders. However, the more general Eq. (10) remains preferable, as it yields precise values of the contact force for arbitrary aspect ratios without increasing the complexity of implementation.

In a recent paper [7] another formula was derived for the contact force, which adapted to our notation and corrected for a typo (in Eq. (17a,17b) of [7], a "2" should be at the denominator of the first term in parentheses rather than an "a" [11]) reads as follows:

$$(F_0)_{AA} = -2\pi K_d R^2 \tau\left(\frac{1}{\sqrt{1+4\tau^2}} + \frac{1}{32\sqrt{(1+4\tau^2)^5}} - \frac{3(3+16\tau^2)}{32\sqrt{(1+4\tau^2)^9}}\right). \tag{12}$$

In the paragraph where we report our experimental measurements, we will also show that both formulas (10) and (12) give values close to the measured contact forces. However, (12) was derived within a somewhat different approximation than (10),

and this becomes particularly evident when τ is small: in the limit $\tau \to 0$, the contact force per unit volume predicted by (12), that is $3/4\ K_d/R$, is just about 85% of the value predicted by (10), that is $4\log(2)/\pi\ K_d/R$. At this stage, it is difficult to assess which of the two formulas is closer to reality. To ascertain which of the two may be deemed "more correct", we will compare both with experimental results in Section 3.

2.2. Two laterally displaced cylindrical permanent magnets

The arrangement of magnets is shown in Fig. 1b. The distance between axes (lateral displacement) is denoted as r. In this case, the magnetostatic energy is

$$E(r,\varsigma) = 8\pi K_d R^3 \int_0^{+\infty} J_0\left(\frac{rq}{R}\right)\frac{J_1^2(q)}{q^2}\sinh(q\tau_1)\sinh(q\tau_2)e^{-q\varsigma}\,dq. \quad (13)$$

The energy gradient, i.e. the force, is then

$$F_z = -8\pi K_d R^2 \int_0^{+\infty} J_0\left(\frac{rq}{R}\right)\frac{J_1^2(q)}{q}\sinh(q\tau_1)\sinh(q\tau_2)e^{-q\varsigma}\,dq, \quad (14)$$

or in an equivalent form

$$F_z = -2\pi K_d R^2 \int_0^{+\infty} J_0\left(\frac{rq}{R}\right)\frac{J_1^2(q)}{q}\sum_{i,j=-1}^{1} i\cdot j\cdot e^{-q(\varsigma+i\tau_1+j\tau_2)}\,dq. \quad (15)$$

For $r=0$ (the common axis case), Eq. (15) transforms into Eq. (4).

In summary, for deriving (14) or (15) we assume uniform magnetization that does not rotate in the presence of other magnets. However, we fully take shape effects into account. In this respect, no approximations were made in deriving the equations. Eq. (14) is the key formula of this study: it is valid for any distance between magnets and for any aspect ratio. Only in some special cases it is worthwhile estimating the integral in (14) with further approximations. A special case of interest is when the axial distance between magnets in question is several times larger than the magnet radius.

If the cylindrical magnets are far from each other, we may find an approximation of the integral in (15) by expanding the Bessel functions around $q=0$ according to their definitory power series [12]. Then, by using $\zeta = (t_1+t_1)/(2R)+x/R$, where x is the gap between the magnets (see Fig. 1), we obtain

$$F_z \approx -\frac{1}{2}\pi K_d R^4 \sum_{i,j=0}^{1}\frac{(-1)^{i+j}}{(x+it_1+jt_2)^2}\left[1-\frac{3}{2}\frac{r^2}{(x+it_1+jt_2)^2}\right]. \quad (16)$$

If, additionally, $t_1=t_2=t$ and $r=0$ then (16) turns into

$$F_z \approx -\frac{1}{2}\pi K_d R^4\left[\frac{1}{x^2}+\frac{1}{(x+2t)^2}-\frac{2}{(x+t)^2}\right]. \quad (17a)$$

Eq. (17a) gives the approximate force between two distant identical cylindrical magnets with the vectors of magnetization lying on their common axis. Fig. 2 shows a comparison between the force approximation (17a) and the exact force (4) for various magnet distances, while we used permanent magnets with the following parameters: $R=1.5$ mm, $t=3$, 6, 9 mm and $M=0.859$ MA/m (corresponding to $K_d=0.463$ MJ/m^3). Eq. (17a) gives an erroneous approximation for small distances between the magnets as the force values become large for close-to-zero distance. However, for distances larger than a certain limit both the respective formulas give force values that are fairly close to each other. Eq. (17a) may be further simplified using

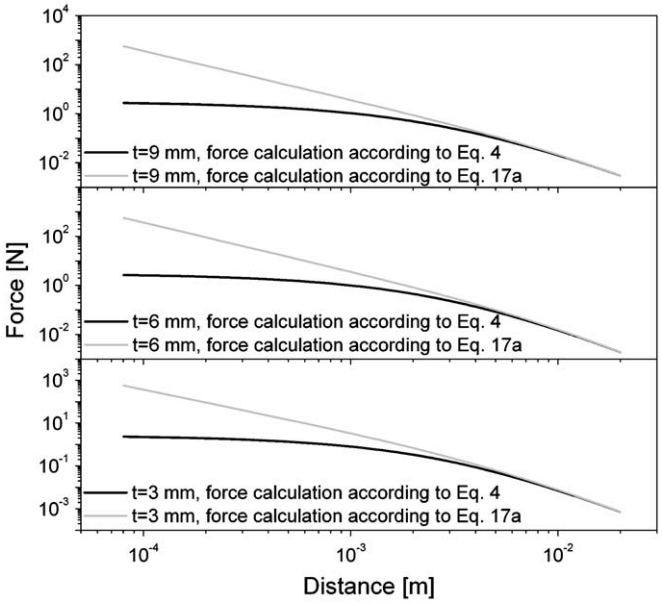

Fig. 2. A comparison between the force approximation, (17a), and the force calculated according to Eq. (4), as a function of the distances between magnets (gap parameter x in Fig. 1). The permanent magnets used have parameters: $R=1.5$ mm, $t=3$, 6, 9 mm and saturation magnetization $M=0.859$ MA/m.

$(1+\varepsilon)^{-2}\approx 1-2\varepsilon+3\varepsilon^2$ for small ε. If $t<x$, we arrive at

$$F_z \approx -3\pi K_d R^4 t^2\frac{1}{x^4}. \quad (17b)$$

This approximation corresponds to the situation when the cylindrical magnets are replaced by dipoles, and is of very limited validity. On the other hand, it is important to confirm that the starting expression (15) has the expected $1/x^4$ asymptotic behavior.

2.3. More than two cylindrical permanent magnets

The calculation of the attraction force between two sets of magnets where either set has more than one magnet is rather complex. If the permanent magnets in the first [second] group are indexed 1, 2, …, n [n+1, n+2, …, m] then the magnetostatic energy of interaction between the two groups reads as follows:

$$E = \sum_{i=1}^{n}\sum_{j=n+1}^{m} E_{ij}(r_{ij},\zeta), \quad (18)$$

where E_{ij} is the interaction energy between magnets i and j, and r_{ij} is their lateral separation. Then, the attraction force along z between the two groups is as follows:

$$F_z = -8\pi K_d R^2 \sum_{i=1}^{n}\sum_{j=n+1}^{m}\int_0^{+\infty} J_0\left(\frac{r_{ij}q}{R}\right)\frac{J_1^2(q)}{q}\sinh(q\tau_i)\sinh(q\tau_j)e^{-q\varsigma}\,dq. \quad (19)$$

2.4. A special case of permanent magnet arrangement with four magnets in the set

Using (19), we can solve any case of permanent magnet arrangement in either set that comply with the above-mentioned assumptions. The case of permanent magnet arrangement we study is shown in Fig. 3. Either set consists of four identical magnets perpendicularly magnetized. Each cylindrical magnet in

the first set has its counterpart in the other set—cylindrical magnet with which it has a common axis and the same orientation of the magnetization vector. In either set, first-neighbor magnets have their magnetization anti-parallel. Since the magnets in each set are touching, the magnet axis distances (r_{ij}) are either $2R$ or $2\sqrt{2}R$. Then according to (19) we arrive at

$$F_z = -32\pi K_d R^2 \int_0^{+\infty} [1 - 2J_0(2q) + J_0(2\sqrt{2}q)] \frac{J_1^2(q)}{q} \sinh^2(q\tau) e^{-q\zeta}\, dq. \tag{20}$$

It is worth noting that the resulting attraction force between the sets shown in Fig. 3 can be larger than four times the attraction force between just two magnets. This is because the anti-parallel overall configuration is substantially more stable energetically than if the four magnets' magnetizations were all aligned. Generally, it is interesting to study the case when the group of four magnets is periodically repeated and fills in an infinite layer. This case will be analyzed elsewhere.

Some approximations of attraction force in (20) may be useful for the case if the magnet sets are far from each other. In this case, we find an approximation of the integral in (20) by expanding the Bessel functions around $q = 0$: $1 - 2J_0(2q) + J_0(2\sqrt{2}q) \approx 0.5q^4$ and $J_1(q) \approx 0.5q$. Substituting $\zeta = (t+x)/R$ we obtain

$$F_z \approx -120\pi K_d R^8 \left[\frac{1}{x^6} + \frac{1}{(x+2t)^6} - \frac{2}{(x+t)^6}\right], \tag{21}$$

and if $t < x$ we finally get

$$F_z \approx -7!\pi K_d R^8 t^2 \frac{1}{x^8}. \tag{22}$$

Fig. 4 shows the diagram of the calculated attraction force versus the distance between sets of magnets that illustrates how the attraction force decreases with different powers of $1/x$ depending on the cylindrical magnet arrangement. The case of arrangement as in Fig. 3 is also included: the corresponding force decreases as $1/x^8$, while in the case of two cylindrical magnets with a common axis the attraction force decreases as $1/x^4$.

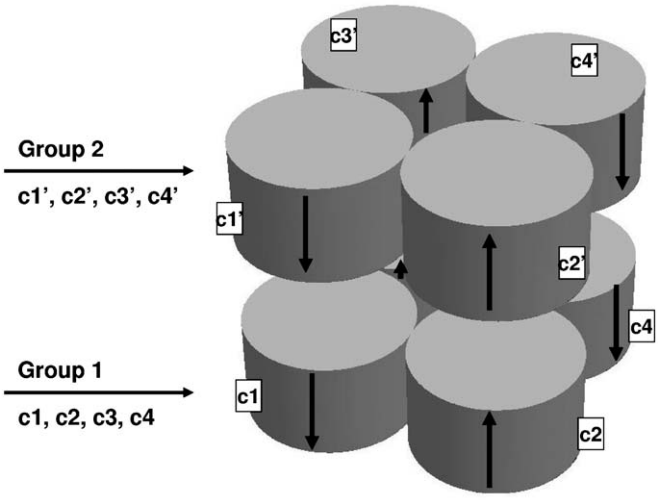

Fig. 3. A scheme of two sets of identical cylindrical permanent magnets. The arrows show the orientation of magnetization. All the magnetization vectors and cylinder axes are parallel.

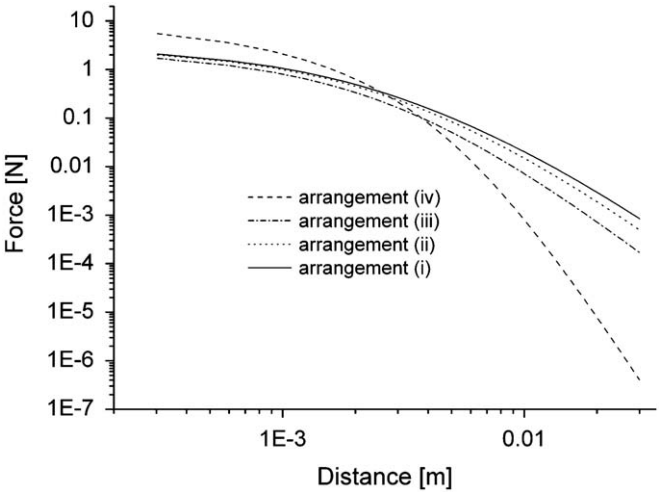

Fig. 4. A diagram of the calculated attraction forces versus distance for various magnet arrangements (the individual arrangements are described in part 3). The magnets diameter and height are 3 and 1.5 mm, respectively, and saturation magnetization equal to 0.859 MA/m.

3. Experimental results

We use NdFeB permanent magnets purchased directly from their manufacturer Elidis sro. Our measurement of magnetic induction with a gaussmeter (F.W.Bell, Model 6010) and Hall-effect probe (STD61-0202-05) yields $B = (1.079 \pm 0.008)T$, corresponding to a saturation magnetization $M = (0.859 \pm 0.006)$ MA/m. The magnets are shaped as cylinders with a diameter of $2R = 3$ mm and a height $t = 1.5$ mm. They are magnetized axially by the producer. The attraction force measurements are carried out at room temperature with a tensile testing machine equipped with a 100 N load cell (HBM, Type S2). Fig. 5 shows the experimental setup for the measurements. The magnets are attached to non-magnetic holders. The holders with the magnets are clamped into the device claws with an effort to have the magnets aligned well (parallel axis and the contact area forms a common base). A small misalignment may result in discrepancy between measured and calculated force values.

In the first stage of the force measurement, force is set to zero when the magnets are far enough from each other. In the second stage, the magnets approach each other until the force drops to zero. At the moment of zero force, the displacement is set to zero. In the third stage, the magnets are slowly pulled away from each other while measuring force and stroke.

The magnets arrangements are:

(i). Either set is formed by two permanent magnets; all the magnets have a common axis.
(ii). Either set is formed by four permanent magnets with a common base. All magnets have a common axis.
(iii). Either set contains six permanent magnets stacked into a longer cylinder of height $t = 9$ mm. All the magnets have again a common axis.
(iv). The sets arrangement is sketched in Fig. 3; the first [second] set is formed by cylindrical magnets c1, c2, c3, c4 [c1′, c2′, c3′, c4′].

Fig. 6 shows a comparison between the measured attraction force and the force calculated from (4) for the cases (i–iii). The force calculation for cases (i–iii) is carried out treating each set as a single cylindrical magnet with height equal to the appropriate multiple of the height of the purchased magnet ($t = 3$, 6 and

9 mm). We obtained a very good agreement between the measured and the calculated forces.

Table 1 summarizes the values of the measured contact forces and the contact forces calculated according (10) and (12). Uncertainties in the calculated values are assigned on the basis of the experimental error associated to the saturation magnetization of the magnets. More specifically, since M was measured with a 0.7% relative error, and the force depends on M^2, we assign a 1.4% relative error to the theoretical predictions.

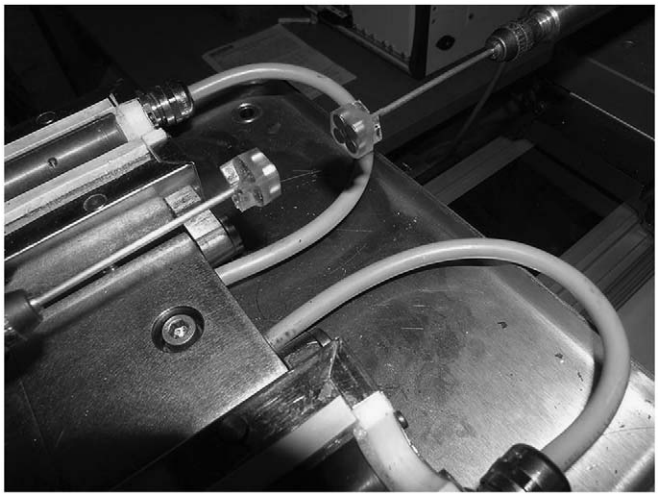

Fig. 5. A photograph of the experimental apparatus for the attraction force measurement.

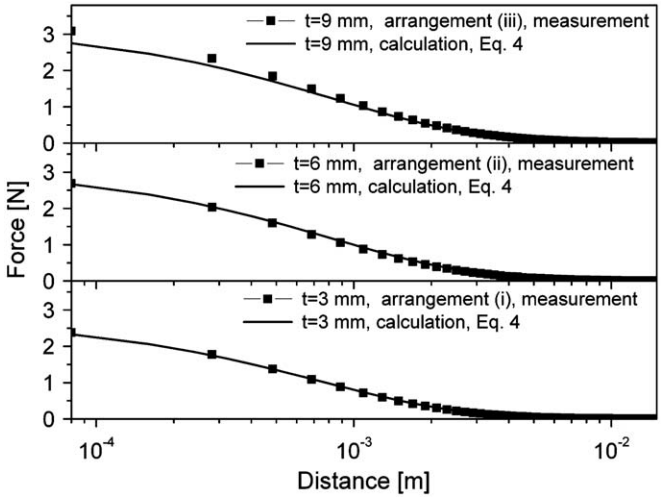

Fig. 6. A diagram of the calculated and measured attraction force versus distance (gap parameter x in Fig. 1) for the magnets of various lengths, $t = 3, 6, 9$ mm with a diameter of 3 mm and saturation magnetization equal to 0.859 MA/m.

Table 1
Measured and calculated contact forces according to (10) and (12) (expression acquired from Ref. [7]).

Magnet shape	Measured contact force [(N])	Contact force [N] according to (10)	Contact force [(N]) according to (12)
$R = 1.5$ mm, $\tau = 1$	2.63 ± 0.03	2.76 ± 0.04	2.92 ± 0.04
$R = 1.5$ mm, $\tau = 2$	2.91 ± 0.03	3.11 ± 0.04	3.18 ± 0.04
$R = 1.5$ mm, $\tau = 3$	3.40 ± 0.03	3.20 ± 0.05	3.23 ± 0.05

The saturation magnetization is equal to 0.859 MA/m.

Both formulas (10) and (12) give values reasonably close to the corresponding measurements. Deviations are expected because theoretical predictions are based on the uniform magnetization approximation, and the geometry where magnets are in close proximity is the most sensitive on non-uniformities/multipoles. On the other hand, we do not expect deviations that are too large, because when magnets are in close proximity they reinforce their respective uniformity near their contact poles. In other words, the contact geometry is a Helmholtz-coil setup, where the field in the vanishing gap is known to be rather uniform.

On the basis of the measurements we carried out, it turned out impossible to determine whether the Agashe–Arnold formula (12) or our Eq. (10) is a more realistic description of the contact force. Predictions of both formulas, for the geometry considered, are within the experimental error, and differ from the experimental values by roughly the same amount. While Eq. (10) appears to be a tiny bit closer to the experiments in the first two cases reported in Table 1, Eq. (12) seems slightly better in the third case. We also note that deviations do not appear systematic: predictions overestimate the measurement in the first two cases, while they underestimate the contact force in the third case.

To compare further the two theoretical predictions beyond the range of aspect ratios available in the experiments, we plot in logarithmic scale the absolute value of the contact force per unit volume (measured in K_d/R) as predicted by formulas (10) and (12). The comparison is shown in Fig. 7, where the experimentally available aspect ratios are indicated by vertical dashed lines. Inspection of the plot reveals the AA-formula (12) deviates substantially from (10) as soon as the aspect ratio is below 1. While (10) goes monotonically to the asymptotic value of $4\log(2)/\pi = 0.883$ when $\tau = 0$, (12) appears to cross a maximum (0.776 for $\tau = 0.225$, which happens to be very close with the only intersection between the two curves occurring at $\tau = 0.252$), and then slowly decreases to its asymptotic value of $3/4 = 0.750$ when $\tau = 0$. Since there is no physical reason justifying the functional behavior of (12) when the aspect ratio approaches zero, we conclude that the maximum, as well as the different asymptotic value, are a result of approximations inherent in the formalism adopted in [7] ceasing to be physically sound. In this respect, we can claim that (10) is a better approximation to reality than (12), in spite of the very close predictions in Table 1 that were more a result of the limited range of aspect ratios we were able to explore experimentally than an actual similarity between the formulas' predictions.

Fig. 8 shows a comparison between the measured attraction force and the force calculated from (20) for the magnet

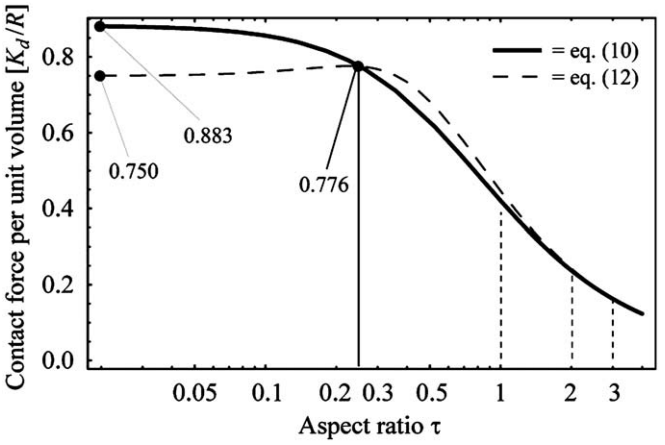

Fig. 7. A diagram of the contact force per unit volume (measured in K_d/R) as predicted by formulas (10) and (12) for various aspect ratios τ.

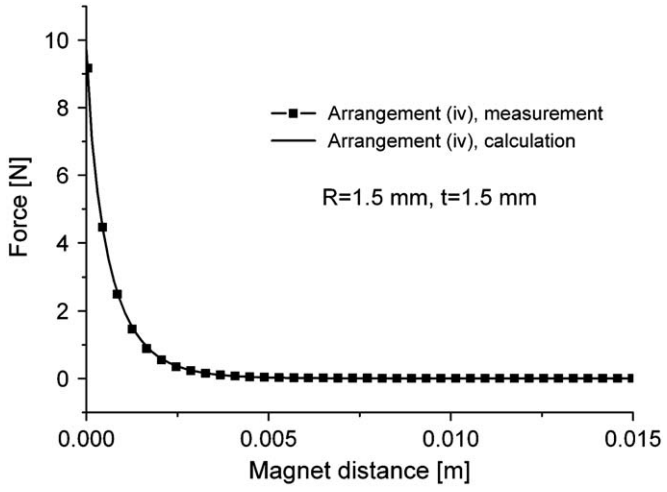

Fig. 8. A diagram of the calculated and measured attraction forces versus distance of the magnets arrangement shown in Fig. 3. The magnets diameter and height are 3 and 1.5 mm, respectively, and saturation magnetization equal to 0.859 MA/m.

arrangement (iv). Also, in this case the agreement between the measured and the calculated forces is more than satisfactory. The largest deviation, barely visible in the figure, is again observed when the magnets are in contact.

4. Conclusions

We have presented formulas for calculating attraction forces between two cylindrical permanent magnets or two sets of permanent magnets on the assumptions of: (i) uniform magnetization in each cylinder and (ii) parallel magnetization directions and magnet axes. For the case of long distance interaction, we re-obtained a simple formula, sometimes utilized in the literature, which approximates the force between permanent magnets. The attraction force measurements were carried out at room temperature combining suitably a series of NdFeB magnets with a diameter of 3 mm and a height of 1.5 mm. The measured force was in excellent agreement (below 1%) with that calculated using our expressions in spite of the seemingly unrealistic assumption of uniform magnetization, except when the gap between sets was very small (contact force) where deviations were closer to 5%. The difference between the measured and the calculated contact forces (Table 1) may be explained by a combination of: (i) non-perfect magnet alignment when measuring forces, (ii) using a stack of magnets rather than a single longer one, (iii) spread in the saturation magnetization of each individual magnet, and (iv) the simplifying assumption of uniform magnetization in the cylindrical magnets.

Acknowledgments

DV acknowledges support by a Marie Curie International Reintegration Grant within the 6th European Community Framework Programme. MB acknowledges the Royal Society for financial support. We acknowledge with gratitude valuable comments and remarks by R. Dunin-Borkowski.

References

[1] M. Beleggia, S. Tandon, Y. Zhu, M. De Graef, J. Magn. Magn. Mater. 278 (2004) 270–284.
[2] M. Beleggia, M. De Graef, J. Magn. Magn. Mater. 285 (2005) L1–L10.
[3] M.E. Schabes, A. Aharoni, IEEE Trans. Magn. 23 (1987) 3882–3888.
[4] H. Fukushima, Y. Nakatani, N. Hayashi, IEEE Trans. Magn. 34 (1998) 193–198.
[5] D. Vokoun, M. Beleggia, T. Rahman, H.C. Hou, C.H. Lai, J. Appl. Phys. 103 (2008) 07F520.
[6] M. Beleggia, D. Vokoun, M. De Graef, J. Magn. Magn. Mater. 321 (2009) 1306–1315.
[7] J.S. Agashe, D.P. Arnold, J. Phys. D: Appl. Phys. 41 (2008) 105001.
[8] D. Craik, Magnetism—Principles and Applications, Wiley, New York, 1995.
[9] G. Eason, B. Noble, I.N. Sneddon, Philos. Trans. R. Soc. London A 247 (1955) 529.
[10] A.P. Prudnikov, Yu.A. Brychkov, O.I. Marichev, Integrals and Series, Volume 2: Special FunctionsGordon and Breach Science Publishers, 1998.
[11] D. Arnold, Personal Communication, 2009.
[12] M. Abramowitz, I. Stegun, Handbook of Mathematical Functions, Dover, New York, 1970, p. 360.